



## Epithelial sodium channel modulates platelet collagen activation



Doris Cerecedo <sup>a,\*</sup>, Ivette Martínez-Vieyra <sup>a</sup>, Lea Alonso-Rangel <sup>a</sup>,  
Claudia Benítez-Cardoza <sup>b</sup>, Arturo Ortega <sup>c</sup>

<sup>a</sup> Laboratorio de Hematobiología, Escuela Nacional de Medicina y Homeopatía (ENMH), Instituto Politécnico Nacional (IPN), Mexico City, Mexico

<sup>b</sup> Laboratorio de Bioquímica, Escuela Nacional de Medicina y Homeopatía (ENMH), Instituto Politécnico Nacional (IPN), Mexico City, Mexico

<sup>c</sup> Departamento de Genética y Biología Molecular, Centro de Investigación y de Estudios Avanzados del IPN (Cinvestav-IPN), Mexico City, Mexico

### ARTICLE INFO

#### Article history:

Received 23 August 2013

Received in revised form 30 January 2014

Accepted 24 February 2014

#### Keywords:

Epithelial sodium channel (ENaC)

Amiloride (AMR)

Adhered platelets

Intermediate filaments (IF)

Dystrophin-associated proteins (DAP)

Platelet migration

### ABSTRACT

Activated platelets adhere to the exposed subendothelial extracellular matrix and undergo a rapid cytoskeletal rearrangement resulting in shape change and release of their intracellular dense and alpha granule contents to avoid hemorrhage. A central step in this process is the elevation of the intracellular  $\text{Ca}^{2+}$  concentration through its release from intracellular stores and on throughout its influx from the extracellular space. The Epithelial sodium channel (ENaC) is a highly selective  $\text{Na}^+$  channel involved in mechanosensation, nociception, fluid volume homeostasis, and control of arterial blood pressure. The present study describes the expression, distribution, and participation of ENaC in platelet migration and granule secretion using pharmacological inhibition with amiloride. Our biochemical and confocal analysis in suspended and adhered platelets suggests that ENaC is associated with Intermediate filaments (IF) and with Dystrophin-associated proteins (DAP) via  $\alpha$ -syntrophin and  $\beta$ -dystroglycan. Migration assays, quantification of soluble P-selectin, and serotonin release suggest that ENaC is dispensable for migration and alpha and dense granule secretion, whereas  $\text{Na}^+$  influx through this channel is fundamental for platelet collagen activation.

© 2014 Elsevier GmbH. All rights reserved.

## Introduction

Blood platelets are small anucleated cell fragments derived from megakaryocytes that prevent blood loss after vessel injury by means of adhering to the exposed subendothelial Extracellular matrix (ECM), collagen being the most thrombogenic component (Baumgartner and Haudenschild, 1972). In response to ECM components, platelets undergo fast cytoskeletal reorganization that results in a change of shape, the release of intracellular dense and alpha granule contents, and adhesion to the damaged vessel, thus stopping hemorrhage. Secondary mediators released from the dense and  $\alpha$ -granules strengthen the activated state, recruiting more platelets to the site of injury. Adhesion of platelets to the damaged endothelium promotes the formation of actin-based structures such as filopodia, lamellipodia, stress fibers, and a contractile ring, which that centralize the granules, forming a structure denominated granulomere. Independent of the

signaling pathway triggered by any of the physiological platelet agonists, a sustained and significant increase in intracellular calcium concentration  $[\text{Ca}^{2+}]_i$  occurs. This increase consists of the release of compartmentalized calcium through the store-operated  $\text{Ca}^{2+}$  entry (SOCE) (Alonso et al., 1991) and the entry of extracellular  $\text{Ca}^{2+}$  at the plasma membrane through the stromal interaction molecule (STIM1), a sensor in the dense tubular system, and Orai1, the major store-operated  $\text{Ca}^{2+}$  (SOC) channel in the plasma membrane or the  $\text{Na}^+/\text{Ca}^{2+}$  exchanger (Braun et al., 2009), contributing to hemostatic platelet responses.

The Epithelial sodium channel/Degenerin (ENaC/Deg) family comprises cation-selective ion channels found widely expressed in animals from hydra and nematodes to vertebrates. ENaC are highly selective  $\text{Na}^+$  channels assembled from three homologous subunits termed  $\alpha$ ,  $\beta$ , and  $\gamma$ . These channels are expressed at the apical membrane of  $\text{Na}^+$  transporting epithelia, where they facilitate  $\text{Na}^+$  reabsorption from the luminal space. ENaC-mediated  $\text{Na}^+$  reabsorption in the distal nephron is important for fluid volume homeostasis and control of the arterial blood pressure (Kellenberger and Schild, 2002). In the airways, ENaC contribute to the maintenance of the airway surface-liquid and mucociliary clearance (Mall et al., 2004). ENaC were initially characterized in the apical membrane of native epithelia as highly selective for

\* Corresponding author at: Laboratorio de Hematobiología, Escuela Nacional de Medicina y Homeopatía (ENMH), IPN, Guillermo Massieu Helguera no. 239, Col. La Escalera Ticomán, 07320 México, DF, Mexico. Tel.: +52 55 57 29 63 00x55531.

E-mail address: dcereced@prodigy.net.mx (D. Cerecedo).

sodium over potassium and sensitive to amiloride (Palmer and Frindt, 1986).

ENaC subunits also play a role in the myogenic response, where vascular smooth muscle cells contract in response to stretching (Drummond et al., 2008), suggesting that ENaC is a mechanosensitive channel. Little is known regarding how extracellular signals are transmitted to the pore of the channel and subsequently alter channel gating. It has been proposed that these channels are tethered through their intra- and extracellular regions to the cytoskeleton and the Extracellular matrix (ECM), respectively (Chalfie, 2009).

ENaC subunits possess two membrane-spanning helices (TM1 and TM2), resulting in cytoplasmic amino and carboxyl termini. The cytoplasmic domains have sites that are phosphorylated by specific kinases, bear specific motifs that direct protein–protein and protein–lipid interactions that affect channel gating and/or trafficking, and have sites that may directly influence channel gating or trafficking. In addition, carboxyl termini serve to link the channel to the cytoskeleton by binding  $\alpha$ -spectrin and possibly actin (Copeland et al., 2001). The Dystrophin glycoprotein complex (DGC) is an oligomeric complex involved in both mechanical stabilizing and signaling roles in mediating interactions among the cytoskeleton, membrane, and ECM. It is thought that the DGC provides proper anchoring and/or clustering to ion channels by its direct or indirect binding to ion transport systems at the plasma membrane (Dallop et al., 2003). In addition to dystrophin, dystroglycan and syntrophins are also components of the DPC core. The syntrophin family of adaptor proteins is composed of the following five members: syntrophins  $\alpha$ -;  $\beta$ 1-;  $\beta$ 2-;  $\gamma$ 1-, and  $\gamma$ 2- (Adams et al., 1993). Each syntrophin contains a Post-synaptic density protein-95, a Drosophila disc large tumor suppressor, and a Zonula occludens-1 protein (zo-1) PDZ domain and two Pleckstrin homology (PH) domains. PDZ domains bind to the C-terminal tails of many different classes of transmembrane protein, but can also participate in homotypic interactions with other PDZ domains containing proteins, including neuronal Nitric oxide synthase (nNOS), as well as in the regulation and localization of various ionic channels and membrane-binding proteins (Brennan et al., 1996).

Dystroglycan is a matrix receptor that spans the plasma membrane linking the cytoplasmic components of the DGC to the ECM. Dystroglycan proteolysis produce two subunits, denominated  $\alpha$ -dystroglycan and  $\beta$ -dystroglycan;  $\alpha$ -dystroglycan binds to ECM proteins, including some laminins, perlecan, agrin, and the neurexins (Michele and Campbell, 2003).  $\beta$ -Dystroglycan associates with  $\alpha$ -dystroglycan at the plasma membrane, whereas the  $\beta$ -Dg transmembrane anchors the  $\alpha$ -dg to the cell membrane and is linked to the actin cytoskeleton via dystrophin, or its isoforms, or its parologue, utrophin, providing structural integrity. In addition, Dg is ideally located for transducing signals from the ECM to the inside of cells, in a similar manner to integrins (Illesley et al., 2001).

In platelets, several classes of ion channels have been identified, including Adenosine triphosphate (ATP)-gated P2X1 channels, Orai1 Store-operated  $\text{Ca}^{2+}$  (SOC) channels (Schmidt et al., 2011), voltage-gated  $K_v$ 1.3 channels (McCloskey et al., 2010), ionotropic glutamate receptors of the 2-Amino-3-(3-hydroxy-5-Methylisoxazol-4-yl) Propanoic Acid (AMPA) (Morrell et al., 2008), and kainate subtypes (Sun et al., 2009), and connexin-specific Gap junction (GJ) channels (Vaiyapuri et al., 2012). However, the expression of ENaC in platelets has not been fully characterized, and it is within this context that, in the present communication, we sought to establish its presence, distribution, and association. Confocal analysis showed the redistribution and co-localization of ENaC from resting to adhered platelets from the cytoplasm to the plasma membrane and the granulomere zone. Immunoprecipitation assays indicated that ENaC is associated with desmin and vimentin, as well as with  $\alpha$ -syntrophin. Platelet migration assays, as well as alpha and dense granule secretion, were not importantly disturbed with ENaC

inhibition. In contrast, pharmacological treatment with amiloride severely affected Na influx in collagen-activated platelets. These results demonstrate ENaC expression in platelets and suggest their involvement in platelet activation.

## Materials and methods

### Platelet preparation

Platelets were obtained by venopuncture from healthy donors who had not received any drug during the 10 days prior to sampling and who gave consent for the procedure to be carried out. Blood was immediately mixed with citrate anticoagulant including dextrose at pH 6.5 (93 mM sodium citrate, 70 mM citric acid, and 140 mM dextrose) at a blood:anticoagulant ratio of 9:1. Platelet-rich plasma was obtained from total blood by centrifugation at 100  $\times g$  for 20 min at room temperature, and was subsequently mixed with an equal volume of citrate anticoagulant and centrifuged at 400  $\times g$  for 10 min (White, 1983). The platelet pack was suspended and washed twice with Hank's balanced saline solution (HBSS) without calcium (137 mM NaCl, 5.3 mM KCl, 1 mM  $\text{MgCl}_2$ , 0.28 mM  $\text{Na}_2\text{HPO}_4 \cdot 12 \text{ H}_2\text{O}$ , 0.87 mM  $\text{NaH}_2\text{PO}_4$ , 0.44 mM  $\text{KH}_2\text{PO}_4$ , 4.1 mM  $\text{NaHCO}_3$ , and 5.5 mM glucose) and counted in a hematocytometer.

### Antibodies

Monoclonal antibodies are referred to as mAb, while polyclonal antibodies are denominated pAb.  $\alpha$ -ENaC pAb Catalogue (Cat.) no. sc-21012, actin mAb no. sc-8432,  $\alpha$ -tubulin mAb Cat. no. sc-5286, NOS3 pAb Cat. no. sc-654,  $\alpha$ -syntrophin pAb Cat. no. sc-13757,  $\beta$ -dystroglycan pAb Cat. no. sc-30405, desmin pAb Cat. no. sc-7559, vimentin pAb Cat. no. sc-7557, PYK2 pAb Cat. no. sc-9019, FAK pAb Cat. no. sc-557, and p-Tyrosine (p-Tyr) agarose beads Cat. no. sc-24957 were purchased from Santa Cruz Biotechnology, Inc. (Santa Cruz, CA, USA), while  $\alpha$ -syntrophin pAb (P6) was the kind gift of D. Mornet (Rivier et al., 1997).

### Preparation of inhibitors

A 2- $\mu\text{M}$  Amiloride (AMR) solution (2 $\times$ ) (Sigma Chemical Co., St. Louis, MO, USA) was directly dissolved in HBSS, a 5- $\mu\text{M}/\text{mL}$  KB-R7943 solution (2 $\times$ ), a 10- $\mu\text{M}$  BAPTA solution (2 $\times$ ), a 10- $\mu\text{M}$  PP2 solution (2 $\times$ ), a 10- $\mu\text{M}$  W7 solution (2 $\times$ ), and a 10- $\mu\text{M}$  Genistein (2 $\times$ ) (Tocris-Cookson, Ellisville, MO, USA) was prepared in HBSS from concentrated solutions diluted in Dimethyl sulfoxide (DMSO).

### Treatment of platelets with inhibitors

Resting platelets in suspension were incubated with the same volume of the drugs to obtain the previously mentioned final concentrations of AMR 2  $\mu\text{M}$ , KB-R7943 5  $\mu\text{M}$ , BAPTA (10  $\mu\text{M}$ ), PP2 (10  $\mu\text{M}$ ), W-7 (N-[6-aminohexyl]-5-chloro-1-naphthalenesulfonamide) (10  $\mu\text{M}$ ), Genistein (10  $\mu\text{M}$ ), and  $\text{Na}_3\text{VO}_4$  (1 M) for 60 min at room temperature.

### RNA isolation

Resting platelets were suspended in TRIzol<sup>®</sup> Reagent, and total RNA was isolated according to the product insert.

### Reverse transcriptase-PCR

cDNA was synthesized from total RNA (3 mg) by Oligo (dT) 20 (5 mM) primed reverse transcriptase according to the product insert using ThermoScript<sup>TM</sup> Reverse Transcriptase. Primers for

ENaC $\alpha$  forward (5'-CTTGCGATGATGTACTGGCA-3') and reverse (5'-GGAAGACGAGCTTGTCCGAGT-3'); ENaC $\beta$  forward (5'-GAGCCC-TGCAACTACCGGA-3') and reverse (5'-GCCGAAGGAAGTGCCTTCTC-3'); ENaC $\gamma$  forward (5'-GCCCTGAAGTCCCTGTATGG-3') and reverse (5'-CGGTGGGAGAACTAGGCTG-3') (Shlyonsky et al., 2005) and GAPDH. PCRs were performed in a 25  $\mu$ L total reaction volume (1.1  $\times$  Master Mix Red Taq DNA polymerase, 1.5 mM MgCl<sub>2</sub> and 100 nM of each appropriate forward and reverse primers in an Eppendorf Mastercycler Gradient). An initial cycle step at 94 °C for 5 min was followed by 35 cycles with a 1 min denaturation at 94 °C, 1 min annealing with an initial temperature of 60 °C, 64 °C and 61 °C for ENaC $\alpha$ , ENaC $\beta$  and ENaC $\gamma$ , respectively, followed by 30 s primer extension at 72 °C, followed by 5 min at 72 °C to ensure complete extension. PCR products were visualized by means of a 1.0% (w/v) agarose gel containing ethidium bromide.

#### Transwell® experiments

$2 \times 10^5$  Control or inhibitor-treated platelets were placed on upper chamber of 0.4- $\mu$ m-pore 24-well inserts (Corning, NY, USA). The lower chamber contained lysate platelets (100 ng/mL) or solvent control DMSO in Iscove's modified Dulbecco's medium (IMDM) medium. Platelets were migrated through the membrane for 2 h at 37 °C, were counted with a hemocytometer, and were confirmed using a flow cytometer (BD FACSCalibur; San Jose, CA, USA) in the platelet gate.

#### Serotonin release

Resting platelets ( $2 \times 10^5$ /mL) were incubated in vehicle (DMSO) and in absence of amiloride 2  $\mu$ M and KB-R7943 5  $\mu$ M, and subsequently activated with collagen 10  $\mu$ M for 4 min. Supernatants were collected and processed by Enzyme-linked immunosorbent assay (ELISA) for quantitative detection of serotonin (Enzo Life Sciences, Inc., Ann Arbor, MI, USA) levels according to the manufacturer's instructions. Standards were included. Plates were read at 405 nm on a microplate reader (Molecular Devices, Sunnyvale, CA, USA) using soft-max-Pro software (Molecular Devices). Mean blank reading was subtracted from each sample and each control reading. A standard curve was plotted, and the serotonin concentration in each sample was determined by interpolation from the standard curve. Three independent experiments were performed and average Standard errors of the mean ( $\pm$ SEM) results are presented graphically.

#### Evaluation of sP-selectin

Resting platelets ( $2 \times 10^5$ /mL) were incubated with amiloride 2  $\mu$ M and KB-R7943 5  $\mu$ M and then activated with collagen 10  $\mu$ M for 4 min. Supernatants were collected and processed by Enzyme-linked immunosorbent assay ELISA for quantitative detection of soluble human P-selectin (sP-selectin) (Invitrogen, Camarillo, CA, USA) levels according to the manufacturer's instructions. Standards were included. Plates were read at 450 nm on a microplate reader (Molecular Devices) using soft-max-Pro software (Molecular Devices). Mean blank reading was subtracted from each sample and each control reading. A standard curve was plotted, and the sP-selectin concentration in each sample was determined by interpolation from the standard curve. Three independent experiments were performed and average  $\pm$  SEM results are presented graphically.

#### Immunofluorescence assays

Fixed resting control DMSO platelets and platelets treated with Amiloride (AMR) were allowed to adhere to glass cover slips in

a wet camera for 20 min. Non-fixed resting control platelets and AMR-treated platelets were adhered to glass cover slips in a wet camera for 20 min; non-adhered cells were removed by washing with HBSS, were fixed, and were permeabilized with a mixture of 2% p-formaldehyde and 0.04% NP40 in PHEM solution (100 mM PIPES, 5.25 mM HEPES, 10 mM EGTA, and 20 mM MgCl<sub>2</sub>). Platelets were first incubated with specific primary antibodies diluted in PBS 0.1% Bovine serum albumin (BSA) and incubated for 2 h. Cells were washed with PHEM solution and incubated for 1 h with secondary antibody conjugated to Alexa-Fluor-488 or Alexa-Fluor-568 (Molecular Probes, Life Technologies, Grand Island, NY, USA) and then washed several times with PHEM and mounted in glycerol 80%. Slides were observed using a Leica confocal instrument model TCS-SP5 Mo, lasers were configured to 20% (17% outside) for Argon and 45% for He/Ne 543, and images were taken at 63 $\times$  zoom 7 $\times$  at 1024  $\times$  1024 pixels with an HCX PL APO 63/1.40–0.60 DIL CS oil immersion. Optical sections (z) were performed at 118 nm with one Airy unit. Negative controls included cells incubated with an irrelevant polyclonal antibody and slides were only exposed to secondary antibodies conjugated to the fluorochromes. Likewise, platelets incubated with 0.1% DMSO were processed for 1 h as the solvent control.

#### Western blotting

Lysates from resting and adhered platelets obtained in Sodium dodecyl sulfate (SDS) and  $\beta$ -mercaptoethanol were boiled for 5 min, subjected to 10% SDS-Polyacrylamide gel electrophoresis (PAGE), and transferred onto nitrocellulose membranes using a semi-dry system (Thermo Electron Co., Milford, MA, USA). Membranes were incubated with appropriate primary antibodies, then with Horseradish peroxidase (HRP)-conjugated secondary antibodies visualized using an enhanced chemoluminescence Western blotting analysis system (Santa Cruz Biotechnology, Inc.), and were documented using T-mat G/RA film (Kodak, Rochester, NY, USA). Negative controls comprised transferred strips incubated solely with HRP-conjugated secondary antibodies.

#### Immunoprecipitation assays

Resting and adhered platelets were lysed for 15 min at 4 °C with an equal volume of 2 $\times$  lysis buffer (2 mM EGTA, 100 mM HEPES, 150 mM NaCl, and 2% NP40, pH 7.4) containing a protease inhibitor cocktail. Lysates were incubated for 2 h at 4 °C with the immunoprecipitating antibodies and subsequently incubated overnight with Rec Protein G-Sepharose (Santa Cruz Biotechnology). Immunoprecipitates (Ip) were separated by centrifugation and washed with NP40-free lysis buffer, then re-suspended in 2X sample buffer (125 mM Tris-HCl, 4% SDS, 20% glycerol, 0.01 mg/mL  $\beta$ -mercaptoethanol and bromophenol blue, pH 6.8) and boiled for 5 min. Immunoprecipitated proteins (Ip) and supernatants were analyzed by Western blotting.

#### Glutathione-S-transferase binding assays

Glutathione S-transferase (GST) pull-down assays were performed as previously described (Cerna et al., 2006). To express and purify GST and GST- $\beta$ -dystroglycan, BL21 DE3 bacteria were transformed with pGex-4T1 (Amersham Biosciences Co., Piscataway, NJ, USA) and pGFP- $\beta$ -Dg vectors, respectively. To perform pull-down assays, a similar amount of GST or GST- $\beta$ -Dg fusion protein that was immobilized onto 20  $\mu$ L of glutathione-Sepharose beads was incubated for 2 h at 4 °C on a rotator with 1 mg of resting whole platelet extract prepared in radioimmunoprecipitation assay buffer containing 1% (v/v) Triton X-100 and 0.1% (w/v) Sodium dodecylsulphate (SDS). Beads were recovered by centrifugation at

6000 rpm for 5 min and washed five times with 1 mL ice-cold NETN buffer. Finally, platelet endogenous proteins bound to glutathione-Sepharose were eluted by adding an equal volume of 2X sample buffer and heating at 95 °C, which was then analyzed by SDS-PAGE) and immunoblotting.

#### Sodium influx

The effect of ENaC inhibitor on collagen-activated platelets in  $[Na^+]$  was evaluated; to this end, platelets suspended in 140 mM NaCl, 4.9 mM KCl, 1.2 mM MgCl<sub>2</sub>, 1.4 mM KH<sub>2</sub>PO<sub>4</sub>, 5.5 mM glucose, and 20 mM HEPES (pH 7.4) were exposed to 2 μM amiloride before their activation with 10 μg/mL collagen. Platelets were loaded with sodium-sensitive fluorescent dye SBFI (10 μM) (Life Technologies, Eugene, OR, USA) according to a published technique (Roberts et al., 2004). The time course of the fluorescence emission of platelet cells upon each treatment was recorded using an LS-55 Spectrofluorometer (Perkin-Elmer, Waltham, MA, USA) equipped with a water-jacketed cell holder for temperature control. All experiments were performed using cells with 0.4-cm path length at 25 °C. Excitation wavelengths were either 345 or 385 nm, correspondingly, and the fluorescence emission was collected at 500 nm.

#### Statistical analysis

Data obtained from serotonin and sP-selectin quantification was expressed as ±SEM), and the results are presented graphically. Statistical analysis was carried out with GraphPad Prism for Windows ver5 software (GraphPad Software, Inc., La Jolla, CA, USA). One-way Analysis of variance (ANOVA) with a multiple comparison test (Tukey test) was utilized for data analysis. Statistical significance was defined as  $p < 0.05$ .

## Results

#### ENaC platelet mRNA expression

In order to provide convincing evidence of platelet ENaC expression, we undertook two approaches, an RT-PCR strategy and a Western blot-based detection. Total RNA was extracted from human platelets, and RT-PCR was performed using primers specific to α-ENaC, β-ENaC and γ-ENaC. The products were visualized in an ethidium bromide agarose gel. The primers chosen for the three isoforms yielded the expected bands of 59, 62 and 61 bp for α-ENaC, β-ENaC and γ-ENaC, respectively, and a band of 496 bp for GAPDH (Fig. 1A). Sequencing of these PCR products confirmed the identity as α-ENaC, β-ENaC and γ-ENaC, respectively.

Total lysates of HeLa and MDCK cells, and platelets were probed with anti-α-ENaC polyclonal antibody (Fig. 1B). The α-ENaC antibody detected the expected band migrating at ~75 kDa.

#### ENaC is associated with intermediate filaments in resting and adhered platelets

There is evidence of direct binding between ENaC and cytoskeletal components (Mazzochi et al., 2006). In order to establish the interactions of ENaC and platelet cytoskeleton components, we performed double immunofluorescence staining utilizing an antibody raised against α-ENaC revealed with a secondary antibody, Alexa-Fluor-488. Actin filaments were identified with Tetramethyl rhodamine iso-thiocyanate (TRITC)-phalloidin, microtubules with an α-tubulin antibody, and intermediate filaments via desmin antibody, all labeled with secondary antibody conjugated to Alexa-Fluor-568 in resting and adhered platelets. Suspended and adhered platelets treated with amiloride 2 μM were also processed for

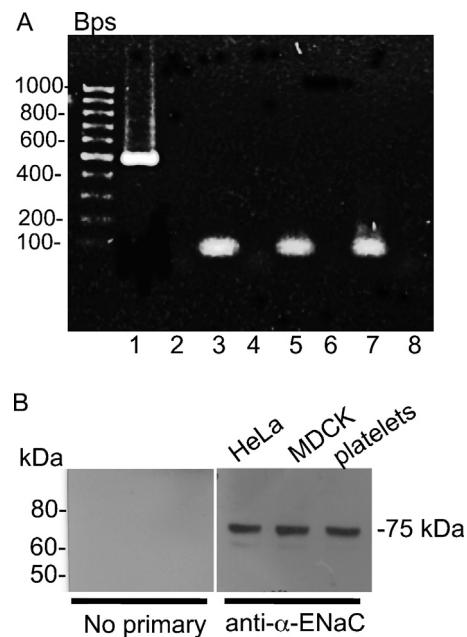


**Fig. 1.** Characterization ENaC in resting human platelets. Panel A. ENaC mRNA expression by PCR. PCR products from human platelets loaded on a 1.2% agarose gel containing ethidium bromide. GAPDH (1), α-ENaC (3), β-ENaC (5), γ-ENaC (7). Lines 2, 4, 6, and 8 corresponded to negative controls. Data are representative from three repeated experiments. Panel B. Western blot analysis of the α-ENaC expression in human platelets. Total lysates protein from HeLa and MDCK cells and human platelets were resolved by western blot and probed with anti-α-ENaC polyclonal antibody revealing the corresponding band of 75 kDa. Controls incubated without primary antibody were included.

triplicate. Negative controls were also included. Confocal analysis showed that in suspension platelets, α-ENaC was distributed in discrete patches at the cytoplasm (Fig. 2, left inset). In adhered platelets, the patched pattern is conserved at the plasma membrane and the cytoplasm is concentrated particularly at the region in which the granules are centralized (granulomere). Platelets have two discrete membrane systems not found in other blood cells: the open canalicular system (OCS), and the dense tubular system (DTS) with no apparent physical communication between them and restricted to one or two areas of the cytoplasm (White, 1999).

In resting platelets, F-actin is observed in clusters around the platelet, while microtubules are organized as concentric rings around the periphery of the platelet; desmin is observed as cytoplasmic thick aggregates. The adhesion process triggers dramatic changes for the three-cytoskeleton elements. F-actin is reorganized into bundles radiating from the granulomere zone in front of the plasma membrane, microtubules were fragmented and redistributed through the cytoplasm, and desmin was observed at the cytoplasm and plasma membrane. Merged images between α-ENaC and cytoskeleton elements showed an apparent co-localization with F-actin and desmin in resting and adhered platelets.

Amiloride partially prevented full spreading, concentrating the presence of α-ENaC at the plasma membrane as patches; platelets that did not fully extend maintained F-actin, microtubules, and desmin with a patched pattern. Apparently, only α-ENaC and desmin proteins partially co-distributed in resting or adhered platelets treated with amiloride.

To corroborate the data observed by confocal analysis, we performed immunoprecipitation assays from control (DMSO), resting, and fully adhered platelet extracts using an α-ENaC antibody. Total (LT) and Ip extracts were resolved by Western blot (Fig. 2B). The results showed that α-ENaC was precipitated only with vimentin

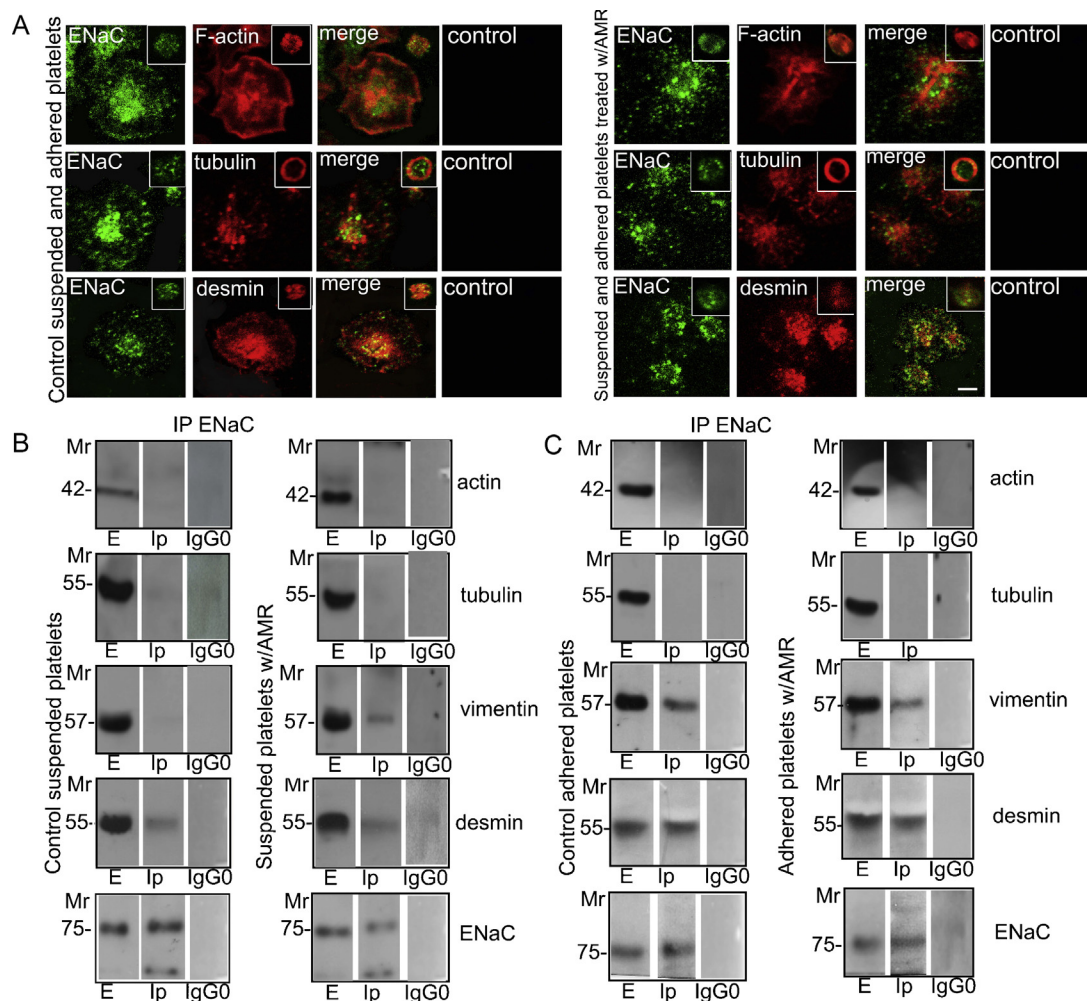


**Fig. 2.** The Epithelial sodium channel (ENaC) is associated with intermediate filaments in resting and adhered platelets. Panel A (left). Control suspended and adhered platelets on glass for 20 min were analyzed by confocal microscopy after processing for double-labeling using antibodies directed against ENaC identified with secondary antibodies labeled with Fluorescein iso-thiocyanate (FITC) and phalloidin labeled with Tetramethyl rhodamine iso-thiocyanate (TRITC), and antibodies directed against  $\alpha$ -tubulin and desmin were revealed with secondary antibodies conjugated to Alexa-Fluor-488. The respective merged images are shown. Scale bar = 1.5  $\mu$ m. Panel A (right). Suspended platelets and settled platelets on glass incubated with Amiloride (AMR) were analyzed by confocal microscopy after processing for double-labeling, employing antibodies directed against ENaC identified with secondary antibody conjugated to Alexa-Fluor-488, and phalloidin labeled with Tetramethyl rhodamine iso-thiocyanate (TRITC), and antibodies directed against  $\alpha$ -tubulin and desmin were revealed with secondary antibodies conjugated to Alexa-Fluor-568. The respective merged images are shown. Controls were performed with only secondary antibodies. Scale bar = 1.5  $\mu$ m. ( $n$  = three independent experiments). Panel B. Control suspended resting and glass adhered platelets for 20 min and suspended resting and glass-adhered platelets treated with AMR (2  $\mu$ M) were processed for immunoprecipitation assays using the anti-ENaC antibody (IP)  $n$  = 3. Proteins from total Extracts (E) and Immunoprecipitates (Ip) were analyzed by immunoblot utilizing antibodies against actin,  $\alpha$ -tubulin, desmin, vimentin, and ENaC. Bands corresponding to desmin, vimentin, and ENaC were detected. None of these proteins were detected in control IgG immunoprecipitates (IgG0 lane). ( $n$  = three independent experiments).

in suspended platelets treated with amiloride, while in adhered platelets  $\alpha$ -ENaC co-precipitated vimentin treated with or without amiloride, in contrast to the bands revealed with desmin that were present in controls or the amiloride in resting and adhered platelets. None of the analyzed proteins was immunoprecipitated with an unrelated IgG0 antibody, confirming assay reliability.

These results showed that desmin is the cytoskeleton element responsible for attaching  $\alpha$ -ENaC to the platelet plasma membrane in suspended and adhered conditions.

#### ENaC is associated with dystrophin-associated protein complex (DAP)

To determine whether pENaC platelets exist with the Dystrophin-associated protein complex (DAPC) as in muscle and brain (Gee et al., 1998), double immunofluorescence was performed in control resting and adhered platelets treated or not with amiloride. Negative controls were also included. ENaC was visualized using a primary antibody revealed with a,

Alexa-Fluor-488 secondary antibody, while  $\beta$ -dystroglycan ( $\beta$ -dg), and  $\alpha$ -syntrophin ( $\alpha$ -syn) were identified using respective primary antibodies revealed with Alexa-Fluor-568 secondary antibodies.  $\alpha$ -Syntrophin displayed a cytoplasmic localization, while  $\beta$ -dystroglycan was mainly located around the plasma membrane in control resting platelets. Under these conditions, there was no co-localization of  $\alpha$ -ENaC and DAPC.

In control adhered platelets,  $\alpha$ -syntrophin and  $\beta$ -dystroglycan showed similar distribution at the plasma membrane and granulomere zone with a patched pattern. Co-localization was clearly observed at the plasma membrane and granulomere suggesting their feasible association.

Confocal microscope analysis of suspended and adhered platelets treated with amiloride showed a punctuate pattern of  $\alpha$ -ENaC and DAPC elements mainly located at the cytoplasm of suspended platelets (Fig. 3A, insets). After the adhesion process  $\alpha$ -ENaC co-distributed with  $\alpha$ -syntrophin at the granulomere zone but not with  $\beta$ -dystroglycan.

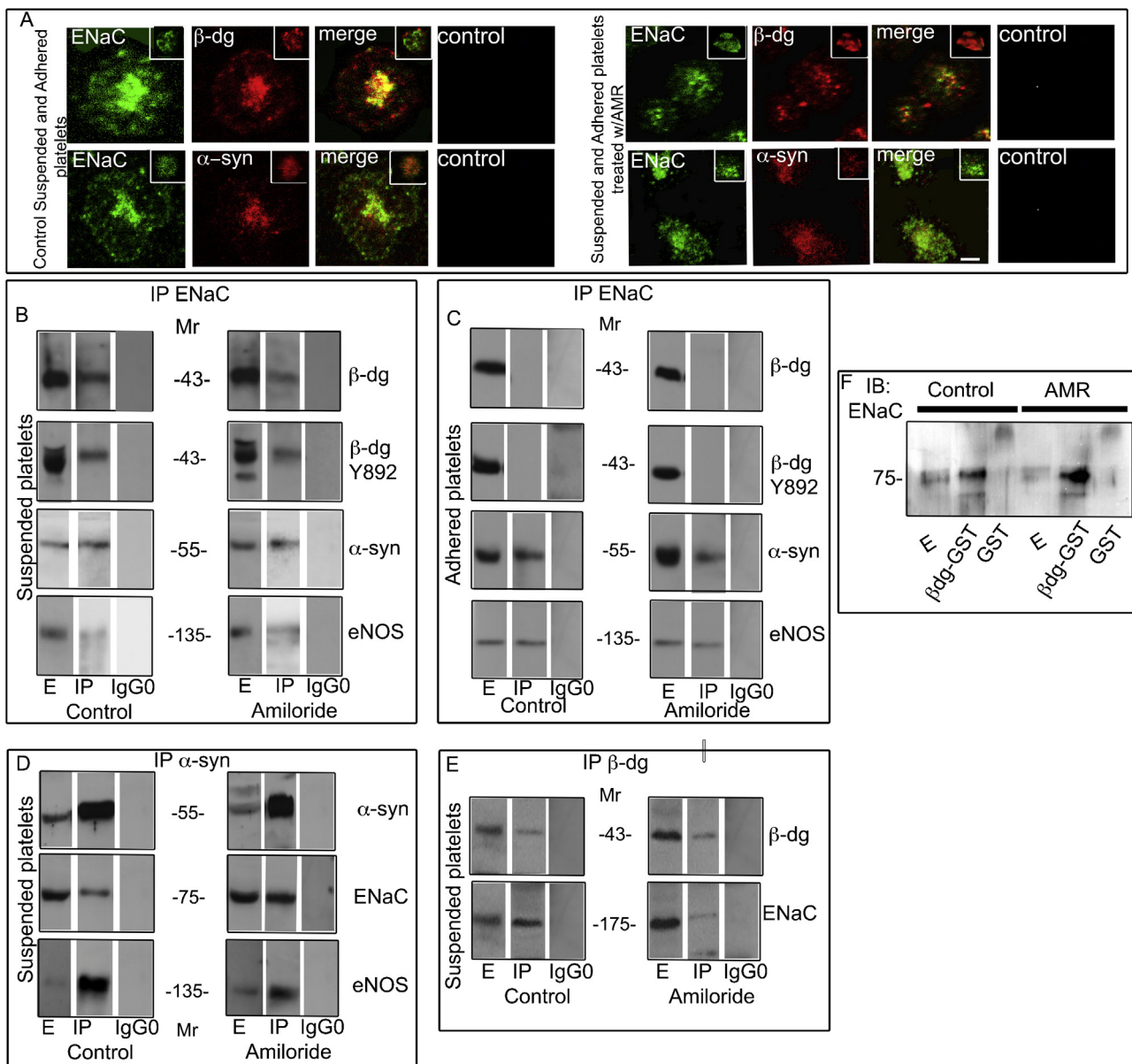


**Fig. 3.** The Epithelial sodium channel (ENaC) is associated with Dystrophin-associated proteins (DAP). Panel A (left). Control suspended and adhered platelets on glass for 20 min were analyzed by confocal microscopy after processing for double-labeling utilizing antibodies directed against ENaC identified with secondary antibodies labeled with secondary antibody conjugated to Alexa-Fluor-488, and antibodies directed against β-dystroglycan and α-syntrophin were revealed with secondary antibodies conjugated to Alexa-Fluor-568. The respective merged images are shown. Scale bar = 1.5 μm. Panel A (right). Suspended platelets and settled platelets on glass incubated with Amiloride (AMR) were analyzed by confocal microscopy after processing for double-labeling, employing antibodies directed against ENaC identified with secondary antibodies labeled with secondary antibody conjugated to Alexa-Fluor-488, and antibodies directed against β-dystroglycan and α-syntrophin were revealed with secondary antibodies conjugated to Alexa-Fluor-568. The respective merged images are shown. Controls were performed with only secondary antibodies. Scale bar = 1.5 μm. ( $n =$  three independent experiments). Panel B. Control suspended resting platelets treated with AMR (2 μM) were processed for immunoprecipitation assays using anti-ENaC antibody (IP). Proteins from total Extracts (E) and Immunoprecipitates (Ip) were analyzed by immunoblot utilizing antibodies against β-dystroglycan, phosphorylated β-dystroglycan phosphorylated (Y892), α-syntrophin, and endothelial Nitric oxide synthase (eNOS). Bands corresponding to β-dystroglycan, phosphorylated β-dystroglycan (Y892), α-syntrophin, and eNOS were detected. None of these proteins were detected in control IgG immunoprecipitates (IgG0 lane) ( $n =$  three independent experiments). Panel C. Control and treated with AMR (2 μM) glass-adhered platelets for 20 min were processed for immunoprecipitation assays using anti-ENaC antibody (IP). Proteins from total Extracts (E) and Immunoprecipitates (Ip) were analyzed by immunoblot utilizing antibodies against β-dystroglycan, phosphorylated β-dystroglycan phosphorylated (Y892), α-syntrophin, and endothelial Nitric oxide synthase (eNOS). Bands corresponding to β-dystroglycan, phosphorylated β-dystroglycan (Y892), α-syntrophin, and eNOS were detected in the Ip fractions but not in fractions obtained with an irrelevant antibody (IgG0). ( $n =$  three independent experiments) Panel D. Control suspended resting and glass-adhered platelets treated with AMR (2 μM) were processed for immunoprecipitation assays using the anti-α-syntrophin antibody (IP). Proteins from total Extracts (E) and Immunoprecipitates (Ip) were analyzed by immunoblot utilizing antibodies against α-syntrophin, ENaC, and endothelial Nitric oxide synthase (eNOS), which revealed the respective bands. None of these proteins were detected in control IgG immunoprecipitates (IgG0 lane). ( $n =$  three independent experiments). Panel E. Control suspended resting and glass-adhered platelets for 20 min and suspended resting and glass-adhered platelets treated with AMR (2 μM) were processed for immunoprecipitation assays using anti-β-dystroglycan antibody (IP). Proteins from total Extracts (E) and Immunoprecipitates (Ip) were analyzed by immunoblot utilizing antibodies against β-dystroglycan and ENaC, which revealed the respective bands with Ip fractions but not in fractions obtained with an irrelevant antibody (IgG0). ( $n =$  three independent experiments). Panel F. *In vitro* interactions of β-dystroglycan (β-Dg) with ENaC were assayed processing Glutathione-S-transferase (GST) and GST-β-Dg proteins isolated from JM109 lysates with glutathione-Sepharose bead. Pulled-down proteins were analyzed by immunoblot assays employing antibodies against ENaC. IB, Immunoblotting.

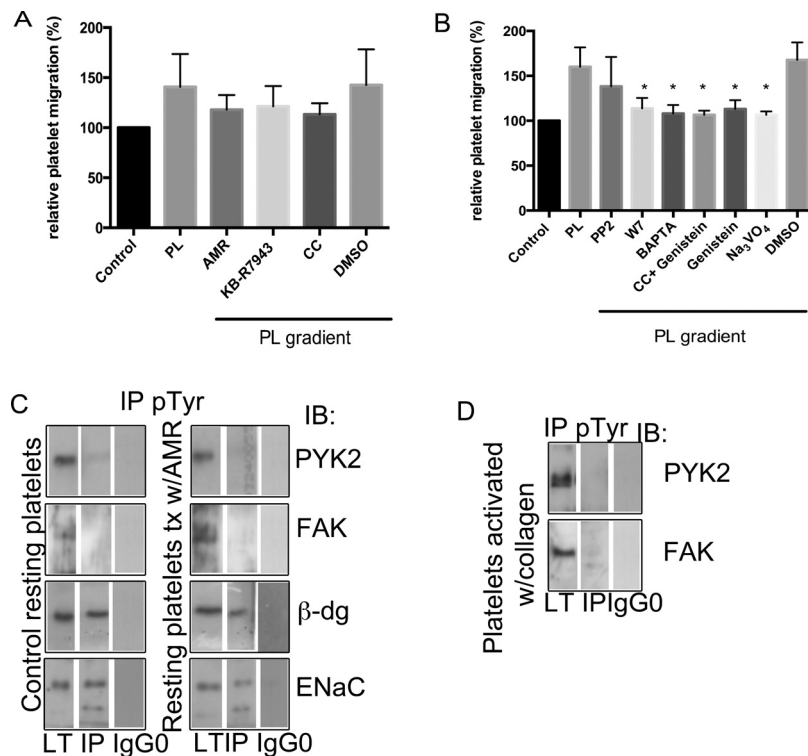


**Fig. 4.** Role of the Epithelial sodium channel (ENaC) in platelet migration. Panel A. Effect on migration of human platelets in the absence and presence of inhibitors. Percentage of platelet migration incubated in the presence or absence of 2 μM Amiloride (AMR), 5 μM KB-R7943, Choline chloride (CC), followed by exposure of Platelet lysate (PL). Arithmetic means ± Standard error of the mean (SEM). (n = three independent experiments). Panel B. Effect on migration of human platelets in the absence and presence of inhibitors. Percentage of platelet migration incubated in the presence or absence of 10 μM PP2, 10 μM W7, 10 μM BAPTA, 10 μM Genistein, 10 μM Genistein in CC buffer, and 1 mM Na<sub>3</sub>VO<sub>4</sub> followed by exposure of PL. Arithmetic means ± SEM. (n = three independent experiments). Panel C. Control suspended resting platelets and platelets treated with AMR were processed for immunoprecipitation assays utilizing pan anti-p-Tyrosine agarose beads (IP, pTyr). Proteins from total Extracts (E) and Immunoprecipitates (Ip) were analyzed by immunoblot utilizing antibodies against PYK2, FAK, β-dystroglycan, and ENaC. None of these proteins were detected in control IgG immunoprecipitates (IgG0 lane). n = 3 Panel D. Collagen activated platelets were processed for immunoprecipitation assays using pan anti-p-tirosine agarose beads (IP, pTyr). Proteins from total extracts (E) and Immunoprecipitates (Ip) were analyzed by immunoblot utilizing antibodies against PYK2 and FAK. None of these proteins were detected in control IgG immunoprecipitates (IgG0 lane). n = 3.

To corroborate the data obtained by confocal microscope, protein extracts of resting and adhered control platelets and treated with amiloride were incubated with anti-ENaC and α-syntrophin antibodies. Western-blot analysis of total extracts and protein immunoprecipitated extracts (Ip) showed that β-dystroglycan and its phosphorylated form were pulled down from ENaC immunoprecipitates of resting control and treated platelets, but not from control or amiloride-treated adhered platelets. In contrast, α-ENaC immunoprecipitated α-syntrophin and endothelial Nitric oxide synthase (eNOS) in control and amiloride treated in suspended and adhered platelets (IP, ENaC) (Fig. 3B and C). Complementary immunoprecipitations performed with α-syntrophin (IP, α-syn) (Fig. 3D) pulled down α-ENaC and eNOS under all conditions assayed. Bands corresponding to ENaC were observed in western blot analysis of β-dg immunoprecipitated proteins in suspended and adhered platelets (IP, β-dg) (Fig. 3E). None of these proteins were detected in control IgG immunoprecipitates (IgG0), confirming assay reliability.

The interaction of α-ENaC with β-Dg, was demonstrated using a GST pull-down assay with a pGex-4T1-derived vector expressing the GST-β-Dg protein fusion. GST or GST-β-Dg fusion protein previously immobilized on glutathione-Sepharose beads was incubated with control suspended platelet extracts, and GST-bound proteins were eluted and analyzed by SDS-PAGE. Immunoblotting with the antibody against α-ENaC exhibited the corresponding band (Fig. 3F).

#### Role of ENaC in platelet migration

To evaluate the feasible role of ENaC in the regulation of platelet migration, we used Transwell® inserts in the presence and absence of Na<sup>+</sup> channel blocker (AMR) 2 μM, Na<sup>+</sup>/Ca<sup>2+</sup> exchanger inhibitor (KB-R7943) 5 μM, and Choline chloride (CC) (Fig. 4A).

Relative transmigrated platelets were counted with a hemocytometer and confirmed by flow cytometer. Our results showed a significant diminution in platelet migration between platelets stimulated with Platelet lysate (PL) in relation to platelets treated with amiloride from mean values of 140.9 to 118%. Additionally, the presence of the Na<sup>+</sup>/Ca<sup>2+</sup> exchanger and in the absence of Na<sup>+</sup> in the buffer solution also significantly diminished platelet migration to 127 and 115%, respectively.

In a second series of experiments, the participation of key elements in platelet migration was assayed. For this purpose, platelets were incubated with a selective intracellular Ca<sup>2+</sup> chelator (BAPTA, 10 μM), an inhibitor of the Src-family (PP2, 10 μM), the calmodulin inhibitor (W7, 10 μM), an inhibitor of tyrosine kinase (Genistein, 10 μM) in the presence and absence of Na<sup>+</sup> and with an alkaline phosphatase and an (Na, K)-ATPase inhibitor (Na<sub>3</sub>VO<sub>4</sub>, 1 μM). The relative migration percentage significantly decreased in platelets treated with [Ca<sup>2+</sup>]<sub>i</sub> chelator (108%) and in platelets exposed to the calmodulin antagonist W7 (114%), to Genistein alone (113%), and to Genistein with Choline chloride (CC) (106%) and Na<sub>3</sub>VO<sub>4</sub> (106%). Interestingly, the Src antagonist did not affect platelet migration (138%) (Fig. 4B).

To further elucidate the biochemical association of tyrosine kinases whether or not migration of platelets were involved, we performed immunoprecipitation assays using a phospho-tyrosine antibody in total lysates from control and platelets treated with amiloride, as well as lysates from collagen-activated platelets. The immunoprecipitated proteins were resolved by Western blot employing antibodies against PYK2, Focal adhesion kinase (FAK),  $\beta$ -dystroglycan ( $\beta$ -dg), and  $\alpha$ -ENaC. None of the analyzed proteins was immunoprecipitated with an unrelated IgG0 antibody, confirming assay reliability. Our results showed that neither PYK nor FAK was phosphorylated under any platelet conditions, in contrast to  $\beta$ -dg and  $\alpha$ -ENaC, which were phosphorylated in control and amiloride-treated platelets.

#### Role of ENaC in platelet granule secretion

To explore the participation of  $\alpha$ -ENaC in granule secretion,  $2 \times 10^5$  resting and collagen-activated platelets/mL were incubated in the presence of AMR,  $\text{Na}^+/\text{Ca}^{2+}$  exchanger (KB-R7943), before platelets were activated with collagen (col) 10 g/mL. Soluble P-selectin and serotonin release represented by the secretion of alpha and dense granules, respectively, were quantified using ELISA kits (Fig. 5A and B).

Serotonin values in control resting platelets were 1.6 ng/mL, which increased when the cells were activated with collagen (10  $\mu\text{g}/\text{mL}$ ) to 24 ng/mL. Surprisingly enough, neither of the treatments (AMR and KB-R7943) were capable of preventing the collagen effect and, in fact, on their own increased serotonin secretion with mean values of 22.8 and 24 ng/mL for collagen-activated platelets treated with AM and KB-R7943, respectively (Fig. 5A).

Release of sP-selectin for control resting platelets was 0.81 ng/mL, while collagen-activated platelets increased sP-selectin levels to a value to 2.3 ng/mL. In similar fashion as to that of serotonin release, neither inhibitor treated blocked the collagen effect (sP-selectin values to 2.47 and 1.33 ng/mL for amiloride and KB-R7943, respectively) (Fig. 5B). Taken together, these results strongly suggest that  $\alpha$ -ENaC is not directly involved in alpha and dense granule secretion.

#### Role of ENaC in collagen-activated platelets

It has been shown that collagen induces an increase in  $[\text{Na}]_i$  (Roberts et al., 2004); therefore, to corroborate the involvement of  $\alpha$ -ENaC in collagen-induced  $\text{Na}^+$  entry, collagen-activated platelets were pre-incubated with amiloride (2  $\mu\text{M}$ ). The samples were excited at 345 or 385 nm and the ratio of fluorescence-emission intensities was registered at 500 nm and plotted in Fig. 6. These relative intensities increased from 2 to 2.37 after platelets were activated with collagen (10  $\mu\text{g}/\text{mL}$ ). In contrast, AMR (2  $\mu\text{M}$ )-treated platelets activated with collagen (10  $\mu\text{g}/\text{mL}$ ) showed a discrete increase of  $[\text{Na}]_i$ , reaching 2.05 fluorescence units (Fig. 6).

#### Discussion

ENaC expression has been previously reported in several tissues, although its functional role(s) within many of them has not been established. In the present study, we demonstrate the expression of  $\alpha$ -ENaC in platelets and, according to our results in collagen-activated platelets, we suggest that  $\text{Na}^+$  dynamics display a two-step process: (1)  $\text{Na}^+$  entry into the cytosolic space via ENaC, and (2)  $\text{Na}^+$  extrusion from the cytosolic space across via the  $\text{Na}^+/\text{Ca}^{2+}$  exchanger (Roberts et al., 2012) and  $\text{Na}^+/\text{H}^+$  exchanger (Tomasiak et al., 2005). It should be noted that amiloride has no effects on platelet  $\text{Na}^+/\text{H}^+$  exchanger (NHE-1) in the range of the concentration used in this work (Siffert et al., 1984).

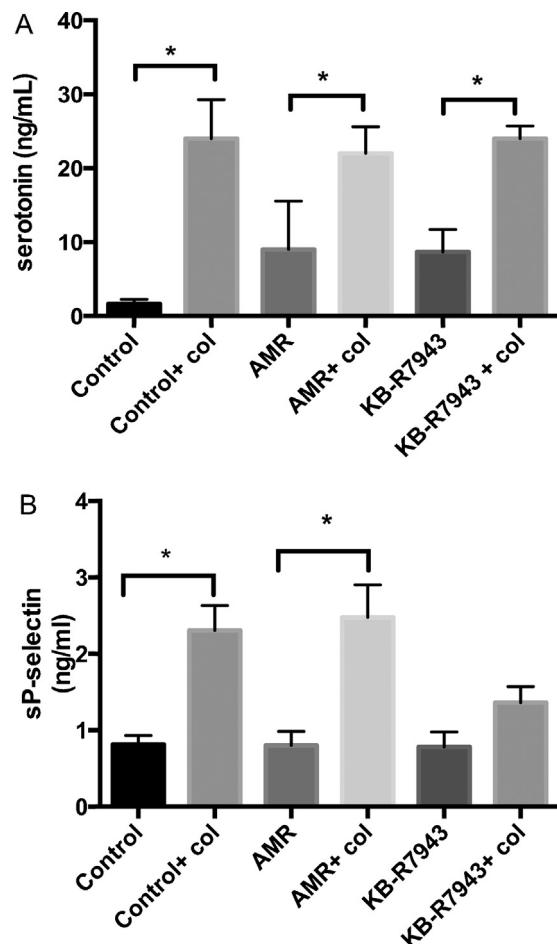


**Fig. 5.** Role of the Epithelial sodium channel (ENaC) in platelet granule secretion. (A) Suspended control and collagen-activated platelets were incubated with vehicle and suspended resting platelets were treated with Amiloride (AMR) (2  $\mu\text{M}$ ), KB-R7943 (5  $\mu\text{M}$ ), Choline chloride (CC), with and without KB-R7943 and Genistein (10  $\mu\text{M}$ ) and further activated with collagen. Supernatants were isolated and quantified for serotonin by Enzyme-linked immunosorbent assay (ELISA) (\* $p < 0.05$ ) ( $n = 3$  independent experiments). Error bars represent Standard error of the mean ( $\pm\text{SEM}$ ). (B) Suspended control and collagen-activated platelets were incubated with vehicle and suspended resting platelets were treated with AMR (2  $\mu\text{M}$ ) and KB-R7943 (5  $\mu\text{M}$ ) and were collagen-activated. Supernatants were isolated and quantified for sP-selectin by ELISA (\* $p < 0.05$ ) ( $n = 3$  independent experiments). Error bars represent  $\pm\text{SEM}$ .

In epithelia and other tissues, ENaC participates in cell migration (Marino et al., 2013) and in wound healing (Chifflet et al., 2005). The basis of this role may involve direct interactions between this protein and cytoskeletal components such as spectrin (Zuckerman et al., 1999) and short actin filaments (Mazzochi et al., 2006). In resting and adhered platelets,  $\alpha$ -ENaC did not co-localize nor associate with actin filaments, microtubules (Fig. 2), or spectrin (data not shown); however, an important association with desmin and vimentin was evident in suspended and adhered platelets (Fig. 2). These results suggest that desmin exerts its scaffolding role, contributing to the maintenance of flexibility and of the regulation of cell shape and cell motility (Helfand et al., 2011). An unexpected observation corresponded to the feasible association of ENaC with vimentin observed only in amiloride-treated platelets but not in control platelets; we speculate that this association could be caused by the alpha subunit conformational change of the ENaC triggered by amiloride (Kashlan and Kleyman, 2011). Cytoskeletal docking restricts ion transport proteins to specialized domains of the plasma membrane, such as syntrophins that interact with several membrane molecules (Gee et al., 1998). In the present study, we

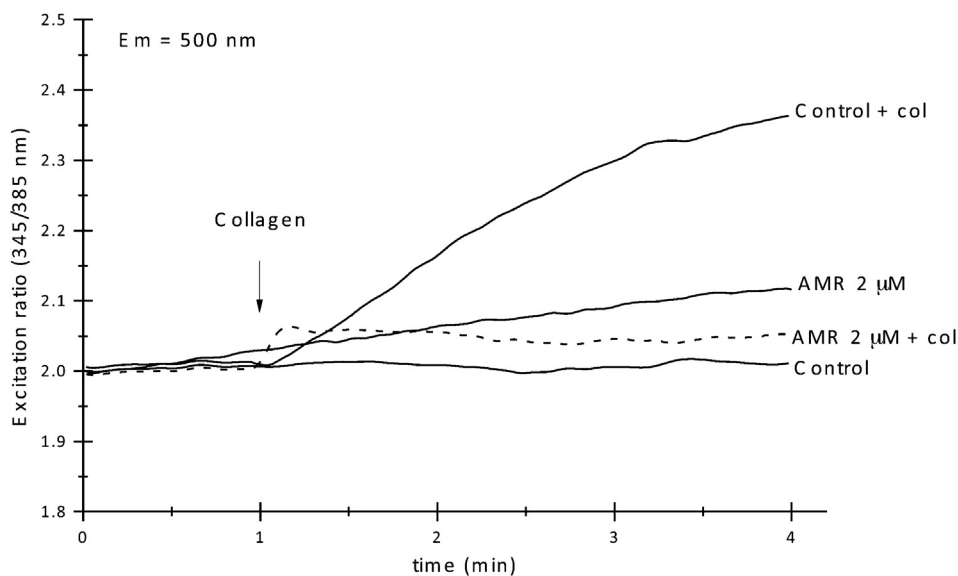


**Fig. 6.** Role of the Epithelial sodium-activated channel (ENaC) in collagen-activated platelets. Effect of Amiloride (AMR) 2  $\mu$ M on collagen-induced change in  $[Na^+]$  triggered by collagen. Ratio fluorescence intensities registered at 345 and 385 nm were plotted.

show that syntrophin is associated with  $\alpha$ -ENaC in suspended and adhered platelets, as well as with eNOS, ensuring its localization in the plasma membrane via the DGC. It is noteworthy that the DGC represents a signaling scaffold for pathways, including Nitric oxide synthase (NOS), PI3-kinase, and Akt, and pathways mediated by means of dystrophin, dystrobrevin, and syntrophins (Zhou et al., 2005).

Dystroglycan represents a physical connection between the ECM and the cytoskeleton and functions as a transducer of signals from outside to inside. Both functions are difficult to discern. In non-muscle cells, it has been identified tyrosine 892 of  $\beta$ -dystroglycan has been identified as an Src and as another Src family kinase substrate, which regulates interaction among dystroglycan and dystrophin and utrophin (James et al., 2000). The association of  $\alpha$ -ENaC with  $\beta$ -dystroglycan in resting platelets, but not in adhered platelets, and specifically its phosphorylated form, indicates that disruption of the interaction of  $\beta$ -dystroglycan with Dp71 and/or utrophin prepares the platelets to trigger shape change or migration, relapsing the stiffness of the cytoskeleton.

It is tempting to speculate that ENaC favors the  $Na^+$  influx that, in turn, triggers the entrance of  $Ca^{2+}$ , resulting in cytoskeletal remodeling during platelet migration. We consider that syntrophins and DGC together help in organizing signaling components that remodel the actin cytoskeleton, as it has been shown that syntrophin recruits signaling proteins, inducing circular ruffles on the membrane (Newey et al., 2000).

Our migration experiments show that ion transport is dispensable for platelet motility because the pharmacological inhibitors of ENaC (amiloride) and a Sodium calcium exchanger (NCX) (KB-R7943) diminish but do not prevent platelet migration. Although actin polymerization at the platelet's leading edge is thought to be a sufficient driving force for membrane protrusion (Borisy and Svitkina, 2000), localized ion fluxes could regulate the activities of proteins that modify actin polymerization, such as cofilin or gelsolin, which are  $Ca^{2+}$ - and pH-sensitive. Platelet migration is affected when two mechanisms that regulate  $Na^+$  entrance through ENaC and NCX 3.2 and NCX 3.4 were inhibited with amiloride or KB-R7943, affecting the increase of  $[Ca^{2+}]_i$  (Roberts et al., 2012).

As in mast cells or in neutrophils, migration is dependent on an increase of intracellular  $Ca^{2+}$  activity, which results from the activation of Orai1, the pore-forming unit of Store-operated  $Ca^{2+}$  entry

(SOCe) (Grosse et al., 2007). Orai1 is also expressed in platelets and is critically important for their activation (Braun et al., 2009). Our results are in accordance with these observations because the use of BAPTA and W7 inhibits platelet migration chelating calcium and inhibiting  $Ca^{2+}$ /Calmodulin protein kinase II (CaMKII), which mediates signaling cascades including the activation of platelet myosin light chain kinase (Hathaway and Adelstein, 1979), suggesting its role in the induction of platelet-shape change (Nachmias et al., 1985). The feasible participation of  $\beta$ -dystroglycan signaling in platelet migration was dismissed because the effect of PP2 (inhibitor of Src) did not modify the platelet migration process.

Platelet agonists perturb the steady state, producing an important increase in cytosolic free  $Ca^{2+}$ , in turn activating multiple signaling events and molecules (Bergmeier and Stefanini, 2009); mediating shape change, secretion of granules, and aggregation (Heptinstall, 1976). Pharmacological inhibition of ENaC and  $Na^+/Ca^{2+}$  exchangers did not diminish serotonin release from dense granules, and these findings are in accordance with other studies that have dismissed the role for NCX or for  $Na^+-Ca^{2+}-K^+$  exchangers (NCKX) in dense granule secretion in human platelets (Shiraga et al., 1998). Blockade of ENaC did not affect sP-selectin liberation from  $\alpha$ -granules; surprisingly enough blockade of and  $Na^+/Ca^{2+}$  exchangers prevented sP-selectin release, but at this stage we do not have a clear explanation for this fact.

Taken together, these results strongly suggest the presence of another  $Na^+$ , not yet identified, channel that is not being inhibited and that might play a key role in granule secretion. In contrast, collagen-induced increase in  $[Na]_i$  was importantly reduced with the pharmacological inhibition of ENaC (amiloride), which strongly suggests that ENaC might be involved in biochemical processes triggered by collagen.

In conclusion, human platelets express  $\alpha$ -ENaC, which is anchored to the plasma membrane through intermediate filaments and, in association with DAP, exerts signaling pathways involved in adhesion, migration, and granule secretion, but specifically in collagen-activation events.

#### Conflict of interest

All the authors stated that they do not have any conflict of interest

## Acknowledgment

The authors thank Iván J. Galván for providing confocal microscopy facilities.

## Appendix A. Supplementary data

Supplementary data associated with this article can be found, in the online version, at <http://dx.doi.org/10.1016/j.ejcb.2014.02.003>.

## References

- Adams, M.E., Butler, M.H., Dwyer, T.M., Peters, M.F., Murnane, A.A., Froehner, S.C., 1993. Two forms of mouse syntrophin, a 58 kd dystrophin-associated protein, differ in primary structure and tissue distribution. *Neuron* 11, 531–540.
- Alonso, M.T., Alvarez, J., Montero, M., Sanchez, A., Garcia-Sancho, J., 1991. Agonist-induced  $\text{Ca}^{2+}$  influx into human platelets is secondary to the emptying of intracellular  $\text{Ca}^{2+}$  stores. *Biochem. J.* 280 (Pt 3), 783–789.
- Baumgartner, H.R., Haudenschild, C., 1972. Adhesion of platelets to subendothelium. *Ann. N. Y. Acad. Sci.* 201, 22–36.
- Bergmeier, W., Stefanini, L., 2009. Novel molecules in calcium signaling in platelets. *J. Thromb. Haemost.* 7 (Suppl. 1), 187–190.
- Boris, G.G., Svitkina, T.M., 2000. Actin machinery: pushing the envelope. *Curr. Opin. Cell Biol.* 12, 104–112.
- Braun, A., Varga-Szabo, D., Kleinschmitz, C., Pleines, I., Bender, M., Austinat, M., Bosl, M., Stoll, G., Nieswandt, B., 2009. Orai1 (CRACM1) is the platelet SOC channel and essential for pathological thrombus formation. *Blood* 113, 2056–2063.
- Brennan, J.E., Chao, D.S., Gee, S.H., McGee, A.W., Craven, S.E., Santillano, D.R., Wu, Z., Huang, F., Xia, H., Peters, M.F., Froehner, S.C., Bredt, D.S., 1996. Interaction of nitric oxide synthase with the postsynaptic density protein PSD-95 and alpha1-syntrophin mediated by PDZ domains. *Cell* 84, 757–767.
- Cerna, J., Cerecedo, D., Ortega, A., Garcia-Sierra, F., Centeno, F., Garrido, E., Mornet, D., Cisneros, B., 2006. Dystrophin Dp71 associates with the beta1-integrin adhesion complex to modulate PC12 cell adhesion. *J. Mol. Biol.* 362, 954–965.
- Chalfie, M., 2009. Neurosensory mechanotransduction. *Nat. Rev. Mol. Cell Biol.* 10, 44–52.
- Chifflet, S., Hernandez, J.A., Grasso, S., 2005. A possible role for membrane depolarization in epithelial wound healing. *Am. J. Physiol. Cell Physiol.* 288, C1420–C1430.
- Copeland, S.J., Berdiev, B.K., Ji, H.L., Lockhart, J., Parker, S., Fuller, C.M., Benos, D.J., 2001. Regions in the carboxy terminus of alpha-bENaC involved in gating and functional effects of actin. *Am. J. Physiol. Cell Physiol.* 281, C231–C240.
- Dallop, C., Sarig, R., Fort, P., Yaffe, D., Bordais, A., Pannicke, T., Grosche, J., Mornet, D., Reichenbach, A., Sahel, J., Nudel, U., Rendon, A., 2003. Targeted inactivation of dystrophin gene product Dp71: phenotypic impact in mouse retina. *Hum. Mol. Genet.* 12, 1543–1554.
- Drummond, H.A., Grifoni, S.C., Jernigan, N.L., 2008. A new trick for an old dogma: ENaC proteins as mechanotransducers in vascular smooth muscle. *Physiology (Bethesda)* 23, 23–31.
- Gee, S.H., Madhavan, R., Levinson, S.R., Caldwell, J.H., Sealock, R., Froehner, S.C., 1998. Interaction of muscle and brain sodium channels with multiple members of the syntrophin family of dystrophin-associated proteins. *J. Neurosci.* 18, 128–137.
- Grosje, J., Braun, A., Varga-Szabo, D., Beyersdorf, N., Schneider, B., Zeitmann, L., Hanke, P., Schropp, P., Muhlstedt, S., Zorn, C., Huber, M., Schmittwolf, C., Jagla, W., Yu, P., Kerka, T., Schulze, H., Nehls, M., Nieswandt, B., 2007. An EF hand mutation in Stim1 causes premature platelet activation and bleeding in mice. *J. Clin. Invest.* 117, 3540–3550.
- Hathaway, D.R., Adelstein, R.S., 1979. Human platelet myosin light chain kinase requires the calcium-binding protein calmodulin for activity. *Proc. Natl. Acad. Sci. U.S.A.* 76, 1653–1657.
- Helfand, B.T., Mendez, M.G., Murthy, S.N., Shumaker, D.K., Grin, B., Mohammad, S., Aebi, U., Wedig, T., Wu, Y.I., Hahn, K.M., Inagaki, M., Herrmann, H., Goldman, R.D., 2011. Vimentin organization modulates the formation of lamellipodia. *Mol. Biol. Cell* 22, 1274–1289.
- Heptinstall, S., 1976. The use of a chelating ion-exchange resin to evaluate the effects of the extracellular calcium concentration on adenosine diphosphate induced aggregation of human blood platelets. *Thromb. Haemost.* 36, 208–220.
- Ilsley, J.L., Sudol, M., Winder, S.J., 2001. The interaction of dystrophin with beta-dystroglycan is regulated by tyrosine phosphorylation. *Cell Signal.* 13, 625–632.
- James, M., Nuttal, A., Ilsley, J.L., Ottersbach, K., Tinsley, J.M., Sudol, M., Winder, S.J., 2000. Adhesion-dependent tyrosine phosphorylation of (beta)-dystroglycan regulates its interaction with utrophin. *J. Cell Sci.* 113 (Pt 10), 1717–1726.
- Kashlan, O.B., Kleyman, T.R., 2011. ENaC structure and function in the wake of a resolved structure of a family member. *Am. J. Physiol. Renal Physiol.* 301, F684–F696.
- Kellenberger, S., Schild, L., 2002. Epithelial sodium channel/degenerin family of ion channels: a variety of functions for a shared structure. *Physiol. Rev.* 82, 735–767.
- Mall, M., Grubb, B.R., Harkema, J.R., O'Neal, W.K., Boucher, R.C., 2004. Increased airway epithelial  $\text{Na}^+$  absorption produces cystic fibrosis-like lung disease in mice. *Nat. Med.* 10, 487–493.
- Marino, G.I., Assef, Y.A., Kotsias, B.A., 2013. The migratory capacity of human trophoblastic BeWo cells: effects of aldosterone and the epithelial sodium channel. *J. Membr. Biol.* 246, 243–255.
- Mazzochi, C., Benos, D.J., Smith, P.R., 2006. Interaction of epithelial ion channels with the actin-based cytoskeleton. *Am. J. Physiol. Renal Physiol.* 291, F1113–F1122.
- McCloskey, C., Jones, S., Amisten, S., Snowden, R.T., Kaczmarek, L.K., Erlinge, D., Goodall, A.H., Forsythe, I.D., Mahaut-Smith, M.P., 2010. Kv1.3 is the exclusive voltage-gated  $\text{K}^+$  channel of platelets and megakaryocytes: roles in membrane potential,  $\text{Ca}^{2+}$  signalling and platelet count. *J. Physiol.* 588, 1399–1406.
- Michele, D.E., Campbell, K.P., 2003. Dystrophin-glycoprotein complex: post-translational processing and dystroglycan function. *J. Biol. Chem.* 278, 15457–15460.
- Morrell, C.N., Sun, H., Ikeda, M., Beique, J.C., Swaim, A.M., Mason, E., Martin, T.V., Thompson, L.E., Gozen, O., Ampagoomian, D., Sprengel, R., Rothstein, J., Faraday, N., Huganir, R., Lowenstein, C.J., 2008. Glutamate mediates platelet activation through the AMPA receptor. *J. Exp. Med.* 205, 575–584.
- Nachmias, V.T., Kavalier, J., Jacobowitz, S., 1985. Reversible association of myosin with the platelet cytoskeleton. *Nature* 313, 70–72.
- Newey, S.E., Benson, M.A., Ponting, C.P., Davies, K.E., Blake, D.J., 2000. Alternative splicing of dystrobrevin regulates the stoichiometry of syntrophin binding to the dystrophin protein complex. *Curr. Biol.* 10, 1295–1298.
- Palmer, L.G., Frindt, G., 1986. Amiloride-sensitive  $\text{Na}^+$  channels from the apical membrane of the rat cortical collecting tubule. *Proc. Natl. Acad. Sci. U.S.A.* 83, 2767–2770.
- Rivier, F., Robert, A., Latouche, J., Hugon, G., Mornet, D., 1997. Expression of a new M(r) 70-kDa dystrophin-related protein in the axon of peripheral nerves from *Torpedo marmorata*. *Comp. Biochem. Physiol. B: Biochem. Mol. Biol.* 116, 19–26.
- Roberts, D.E., McNicol, A., Bose, R., 2004. Mechanism of collagen activation in human platelets. *J. Biol. Chem.* 279, 19421–19430.
- Roberts, D.E., Matsuda, T., Bose, R., 2012. Molecular and functional characterization of the human platelet  $\text{Na}(+)/\text{Ca}(2+)$  exchangers. *Br. J. Pharmacol.* 165, 922–936.
- Schmidt, E.M., Munzer, P., Borst, O., Kraemer, B.F., Schmid, E., Urban, B., Lindemann, S., Ruth, P., Gawaz, M., Lang, F., 2011. Ion channels in the regulation of platelet migration. *Biochem. Biophys. Res. Commun.* 415, 54–60.
- Shiraga, M., Tomiyama, Y., Honda, S., Suzuki, H., Kosugi, S., Tadokoro, S., Kanakura, Y., Tanoue, K., Kurata, Y., Matsuawa, Y., 1998. Involvement of  $\text{Na}^+/\text{Ca}^{2+}$  exchanger in inside-out signaling through the platelet integrin IIb $\beta$ 3. *Blood* 92, 3710–3720.
- Shlyonsky, V., Goolaerts, A., Van Beneden, R., Sariban-Sohraby, S., 2005. Differentiation of epithelial  $\text{Na}^+$  channel function. An in vitro model. *J. Biol. Chem.* 280, 24181–24187.
- Siffert, W., Fox, G., Muckenhoff, K., Scheid, P., 1984. Thrombin stimulates  $\text{Na}^+/\text{H}^+$  exchange across the human platelet plasma membrane. *FEBS Lett.* 172, 272–274.
- Sun, H., Swaim, A., Herrera, J.E., Becker, D., Becker, L., Srivastava, K., Thompson, L.E., Sher, M.R., Perez-Tamayo, A., Suktitipat, B., Matthias, R., Contractor, A., Faraday, N., Morrell, C.N., 2009. Platelet kainate receptor signaling promotes thrombosis by stimulating cyclooxygenase activation. *Circ. Res.* 105, 595–603.
- Tomasik, M., Ciborowski, M., Stelmach, H., 2005. The role of  $\text{Na}^+/\text{H}^+$  exchanger in serotonin secretion from porcine blood platelets. *Acta Biochim. Pol.* 52, 811–822.
- Vaiyapuri, S., Jones, C.I., Sasikumar, P., Moraes, L.A., Munger, S.J., Wright, J.R., Ali, M.S., Sage, T., Kaiser, W.J., Tucker, K.L., Stain, C.J., Bye, A.P., Jones, S., Oviedo-Orta, E., Simon, A.M., Mahaut-Smith, M.P., Gibbins, J.M., 2012. Gap junctions and connexin hemichannels underpin hemostasis and thrombosis. *Circulation* 125, 2479–2491.
- White, J.G., 1983. Ultrastructural physiology of platelets with randomly dispersed rather than circumferential band microtubules. *Am J Pathol* 110, 55–63.
- White, J.G., 1999. Platelet membrane interactions. *Platelets* 10, 368–381.
- Zhou, Y.W., Oak, S.A., Senogles, S.E., Jarrett, H.W., 2005. Laminin-alpha1 globular domains 3 and 4 induce heterotrimeric G protein binding to alpha-syntrophin's PDZ domain and alter intracellular  $\text{Ca}^{2+}$  in muscle. *Am. J. Physiol. Cell Physiol.* 288, C377–C388.
- Zuckerman, J.B., Chen, X., Jacobs, J.D., Hu, B., Kleyman, T.R., Smith, P.R., 1999. Association of the epithelial sodium channel with Apx and alpha-spectrin in A6 renal epithelial cells. *J. Biol. Chem.* 274, 23286–23295.